Therapeutic MK-4482/EIDD-2801 Blocks SARS-CoV-2 Transmission in Ferrets

Robert M. Cox[1#], Josef D. Wolf[1#], Richard K. Plemper[1]*

[1]Institute for Biomedical Sciences, Georgia State University, Atlanta, GA

[#]these authors contributed equally to this work

Short title: Therapeutic Block of SARS-CoV-2 Spread

*to whom correspondence should be addressed: rplemper@gsu.edu

1 **Summary Paragraph**

2   **The COVID-19 pandemic is having a catastrophic impact on human health. Widespread**

3 **community transmission has triggered stringent distancing measures with severe socioeconomic**

4 **consequences. Gaining control of the pandemic will depend on interruption of transmission chains**

5 **until protective herd immunity arises. Ferrets and related members of the weasel genus transmit**

6 **SARS-CoV-2 efficiently with minimal clinical signs, resembling spread in the young-adult**

7 **population. We previously reported an orally efficacious nucleoside analog inhibitor of influenza**

8 **viruses, EIDD-2801 (or MK-4482), that was repurposed against SARS-CoV-2 and is in phase II/III**

9 **clinical trials. Employing the ferret model, we demonstrate in this study high SARS-CoV-2 burden**

10 **in nasal tissues and secretions that coincides with efficient direct-contact transmission.**

11 **Therapeutic treatment of infected animals with twice-daily MK-4482/EIDD-2801 significantly**

12 **reduced upper respiratory tract SARS-CoV-2 load and completely suppressed spread to untreated**

13 **contact animals. This study identifies oral MK-4482/EIDD-2801 as a promising antiviral**

14 **countermeasure to break SARS-CoV-2 community transmission chains.**

Main Text

The coronavirus disease (COVID)-19 pandemic is exerting a global impact on human health not experienced from a single pathogen since the Spanish flu outbreak of 1918. The etiologic agent, SARS-CoV-2, has spread to over 35.5 million people to date, causing over 1 million deaths and substantial morbidity, and having an unprecedented catastrophic effect on societies and the global economy[1]. Interrupting widespread community transmission is paramount to establishing pandemic control and relaxing social-distancing measures. However, no vaccine prophylaxis is yet available and approved antiviral treatments such as remdesivir and reconvalescent serum cannot be delivered orally[2,3], making them poorly suitable for transmission control.

We recently reported the development of MK-4482/EIDD-2801[4,5], the orally available pro-drug of the nucleoside analog N^4-hydroxycytidine (NHC), which has shown potent anti-influenza virus activity in mice, guinea pigs, ferrets, and human airway epithelium organoids[4,6,7]. Acting through induction of error catastrophe in virus replication[4,8], NHC has broad-spectrum anti-RNA virus activity and is currently being tested in advanced clinical trials (NCT04405570 and NCT04405739) for the treatment of SARS-CoV-2 infection. In addition to ameliorating acute disease, we have demonstrated in a guinea pig transmission model that NHC effectively blocks influenza virus spread from infected animals to untreated contact animals[7].

Several mouse models of SARS-CoV-2 infection have been developed, some of which were employed to confirm *in vivo* efficacy of MK-4482/EIDD-2801 also against beta-coronaviruses[9]. However, human SARS-CoV-2 cannot productively infect mice without extensive viral adaptation or introduction of human ACE2 into transgenic animals, and none of the mouse models supports transmission to uninfected mice[10]. Spillover of SARS-CoV-2 to farmed minks, subsequent large-scale mink-to-mink transmission and, in some cases, zoonotic transmission back to humans revealed efficient

38 viral spread among members of the weasel genus without prior adaptation[11-14]. Although mink farms

39 reported elevated animal mortality and gastrointestinal and respiratory clinical signs[15], outbreak follow-

40 up revealed continued intra-colony spread for extended periods of time[14], suggesting that acute clinical

41 signs in the majority of infected animals may be mild or absent. These mink field reports corroborated

42 results obtained with experimentally infected ferrets showing that mustelids of the weasel genus transmit

43 SARS-CoV-2 efficiently without strong clinical disease manifestation[16,17]. This presentation of SARS-

44 CoV-2 infection resembles the experience of frequently asymptomatic or mildly symptomatic SARS-

45 CoV-2 spread in the human young-adult population[18].

46   In this study, we have explored the efficacy of oral MK-4482/EIDD-2801 against SARS-CoV-2 in

47 the ferret model. We demonstrate significant reduction of upper respiratory tract virus load in animals

48 treated therapeutically with MK-4482/EIDD-2801. Whereas SARS-CoV-2 efficiently spread to all

49 contacts of vehicle-treated source animals, MK-4482/EIDD-2801 treatment blocked all SARS-CoV-2

50 transmission. These results support the administration of MK-4482/EIDD-2801 to asymptomatic or

51 mildly symptomatic SARS-CoV-2 positives to rapidly block community transmission chains in addition

52 to the treatment of patients with advanced clinical signs or severe disease.

53 **Efficient replication and shedding of SARS-CoV-2 in the ferret upper respiratory tract**

54   To validate host invasion and tissue tropism of SARS-CoV-2 in ferrets, we inoculated animals

55 intranasally with 1×10^4 or 1×10^5 plaque-forming units (pfu) of SARS-CoV-2 clinical isolate 2019-

56 nCoV/USA-WA1/2020 per animal. Shed virus burden was monitored daily over a 10-day period and

57 virus load in the upper and lower respiratory tract determined on days four and ten after infection. In

58 animals of the high inoculum group, virus release from the upper respiratory tract peaked three days

59 after infection and was undetectable by day seven (Fig. 1a). No efficient infection was noted in the low

60 inoculum group. Shedding profiles closely correlated with infectious particle load in nasal turbinates; a

61   heavy virus tissue burden in the high inoculum group was present on day 4, which greatly decreased by

62   approximately four orders of magnitude by day 10 (Fig. 1b).

63   Low inoculum resulted in light virus load in the turbinates on day 4 and undetectable burden

64   thereafter. However, qPCR-based quantitation of viral RNA copy numbers in the turbinates revealed

65   continued presence of a moderate (approx. 10^4 copies/g tissue) to high ($\geq 10^7$ copies/g tissue) virus load

66   after low and high inoculum, respectively (Fig. 1c). Independent of inoculum amount, no infectious

67   particles were detected in bronchoalveolar lavages or lung tissue samples (extended data Fig. 1). At both

68   days 4 and 10, several organ samples (lung, heart, kidney, liver) were also qPCR-negative (Fig. 1d),

69   confirming inefficient infection of the ferret lower respiratory tract and limited systemic host invasion.

70   Only small and large intestine samples were PCR-positive on day 4 after infection, and rectal swabs

71   showed continued low-grade shedding of viral genetic material (Fig. 1e).

72   Animals in the high-inoculum group experienced a transient drop in body weight that reached a low

73   plateau on days 5-6 after infection, but fully recovered by the end of study (Fig. 1f). No other clinical

74   signs such as fever or respiratory discharge were noted. Complete blood counts taken every second day

75   revealed no significant deterioration from the normal range in either inoculum group in overall white

76   blood cells counts and lymphocyte, neutrophil, and platelet populations (Fig. 1g). Relative expression

77   levels of type I and II interferon and IL-6 in ferret peripheral blood mononuclear cells (PBMCs) sampled

78   in 48-hour intervals reached a plateau approximately 3 days after infection and stayed moderately

79   elevated until the end of the study (Fig. 1h). Selected interferon-stimulated genes (ISGs) with antiviral

80   effector function (MX1 and ISG15) showed a prominent expression peak four days after infection,

81   followed by return to baseline expression by study end.

82   **Efficacy of MK-4482/EIDD-2801 against SARS-CoV-2 in ferrets**

83   Informed by these results, ferrets were infected in subsequent MK-4482/EIDD-2801 efficacy tests

5

84   with 1×10^5 pfu/animal and infectious virions in nasal lavages determined twice daily (Fig. 2a). Viral

85   burden in respiratory tissues was assessed four days after infection. In all treatment experiments, MK-

86   4482/EIDD-2801 was administered twice daily (*b.i.d.*) through oral gavage. Dosing commenced 12

87   hours after infection at 5 or 15 mg/kg body weight, or 36 hours after infection at 15 mg/kg. Shed viral

88   titers in nasal lavages were equivalent in all MK-4482/EIDD-2801 groups and vehicle-treated controls at

89   the time of first treatment start (12 hours after infection), indicating uniform inoculation of all animals in

90   the study (Fig. 2b). Initiation of therapy at the 12-hour time point resulted in a significant reduction

91   ($p<0.001$) of shed virus load within 12 hours, independent of the MK-4482/EIDD-2801 dose level

92   administered, and infectious particles became undetectable within 24 hours of treatment start. When first

93   administered at the peak of virus shedding (36 hours after infection), MK-4482/EIDD-2801 completely

94   suppressed release of infectious virions into nasal lavages within a slightly longer 36-hour period,

95   whereas vehicle control animals continued to shed infectious particles until study end.

96   By 3.5 days after infection, only vehicle-treated animals carried detectable virus burden in nasal

97   turbinates (Fig. 2c), indicating that MK-4482/EIDD-2801 had silenced all SARS-CoV-2 replication.

98   SARS-CoV-2 RNA was still detectable in nasal tissues extracted from animals of all groups, albeit

99   significantly reduced ($p=0.0089$ and $p=0.0081$ for the 5 mg/kg and 15 mg/kg MK-4482/EIDD-2801

100   groups, respectively) in treated animals versus the vehicle controls (Fig. 2d). Animals of the 12-hour

101   therapeutic groups showed a significant reduction ($p\leq0.044$) in effector ISG expression compared to

102   vehicle-treated animals, although no significant differences in relative interferon and IL-6 induction

103   were observed (extended data Fig. 2).

104   These results demonstrate oral efficacy of therapeutically administered MK-4482/EIDD-2801

105   against acute SARS-CoV-2 infection in the ferret model. Consistent with our previous pharmacokinetic

106   (PK) and toxicology work-up of MK-4482/EIDD-2801 in ferrets, treatment did not cause any

107   phenotypically overt adverse effects and white blood cell and platelet counts of drug-experienced

108   animals remained in the normal range (extended data Fig. 3).

109   **Efficient direct contact transmission of SARS-CoV-2 between ferrets**

110   SARS-CoV-2 shedding into the ferret upper respiratory tract establishes conditions for productive

111   spread from infected source to uninfected contact animals[16,17]. To assess transmission efficiency, we co-

112   housed intranasally infected source animals with two uninfected contact animals each for a 3-day period,

113   starting 30 hours after source animal inoculation (Fig. 3a). Nasal lavages and rectal swabs were obtained

114   from all animals once daily and blood sampled at study start and on days four and eight after the original

115   infection. Viral burden and RNA copy numbers in respiratory tissues were determined at the end of the

116   co-housing phase (source animals) and at study end (contact animals).

117   Infectious particles first emerged in nasal lavages of some contact animals 24 hours after the start of

118   co-housing (Fig. 3b). By the end of the co-housing phase, all contact animals were infected and

119   approached peak virus replication phase, demonstrating that SARS-CoV-2 transmission among ferrets is

120   rapid and highly efficient.

121   **MK-4482/EIDD-2801 prevents viral spread to untreated contact animals**

122   A second cohort of source animals inoculated in parallel with SARS-CoV-2 received oral MK-

123   4482/EIDD-2801 at the 5 mg/kg body weight dose level, administered *b.i.d.* starting 12 hours after

124   infection. Productive infection of these animals was validated by SARS-CoV-2 titers in nasal lavages

125   one day after infection (Fig. 3b) that very closely matched those seen in the initial efficacy tests (Fig.

126   2b). Although we also co-housed the treated source animals for nearly 3 days with two untreated

127   contacts each, no infectious SARS-CoV-2 particles were detected in any of the series of nasal lavages

128   obtained from these contacts or in any of the contact animal nasal turbinates sampled at study end (Fig.

129   3c).

130   Nasal turbinates extracted from the contacts of vehicle-treated source animals contained high viral

131   RNA copy numbers, underscoring successful host invasion after transmission (Fig. 3d). Consistent with

132   our earlier observations, turbinates of treated source animals harbored moderate to high ($\geq 10^5$ copies/g

133   tissue) amounts of viral RNA although infectious particles could not be detected. In contrast, all

134   respiratory tissues of the contacts co-housed with MK-4482/EIDD-2801-treated source animals

135   remained SARS-CoV-2 genome free, indicating the absence of any low-grade virus replication that

136   could have hypothetically progressed in these animals below the detection level of infectious particles

137   (Fig. 3e,f). Low SARS-CoV-2 RNA copy numbers were furthermore present in intestine tissue samples

138   and rectal swabs of the vehicle source animals and their contacts, but were undetectable in the MK-

139   4482/EIDD-2801-treated source group and co-housed contact animals.

140

141   **Discussion**

142   Representatives of a number of animal species such as non-human primates[19], dogs[20], cats[20],

143   ferrets[20], hamsters[21-23], and bats[16] were susceptible to SARS-CoV-2 without prior species adaptation

144   when infected experimentally. Natural infection has been documented for felines[24], dogs[25] and

145   minks[12,14]. Phylogenetic analysis of outbreaks in mink farms revealed prolonged intra-colony circulation

146   and zoonotic mink-to-human transmission[14], driving our selection of ferrets, members of the weasel

147   genus closely related to minks, as a relevant SARS-CoV-2 transmission model.

148   We noted strong viral inoculum amount-dependence of experimental infection of ferrets. Productive

149   host invasion characterized by robust virus replication in the upper respiratory tract and appearance of

150   viral genetic material in gastrointestinal samples was only observed after intranasal delivery of 100,000

151   pfu of SARS-CoV-2. By comparison, natural infection through direct contact was far more efficient, to

152   which prolonged exposure of contact to source animals may have been a contributing factor. However,

153 nearly all contacts started to shed virus within less than 24 hours after the beginning of co-housing. This

154 timeline indicates that transmission must have occurred in most cases immediately after introducing

155 contact to source animals, despite the fact that shed viral titers of source animals were only 10^3 pfu/ml

156 nasal lavage in this disease period.

157   Independent of experimental versus natural infection, none of the SARS-CoV-2 infected ferrets

158 displayed prominent clinical signs. The mink farm outbreaks may allow better appreciation of the

159 clinical spectrum of SARS-CoV-2 in weasels, since data are based on a far greater number of animals.

160 Whereas only a small subset of the thousands of infected minks displayed severe respiratory signs, most

161 of those that died at the peak of farm outbreaks had developed acute interstitial pneumonia[12,15]. Possibly

162 a consequence of mild disease in ferrets, our complete blood counts showed no robust lymphopenia, a

163 prominent correlate of severe human SARS-CoV-2 disease[26,27].

164   MK-4482/EIDD-2801 is currently being tested in advanced multi-center clinical trials

165 (NCT04405570 and NCT04405739), which explore drug efficacy in lowering virus shedding in SARS-

166 CoV-2-positive non-hospitalized and hospitalized patients, respectively. These studies were launched

167 after successful completion of phase 1 safety trials (i.e. NCT04392219). Although dose levels applied in

168 these studies and human PK data have not yet been disclosed, Merck & Co. have released[28] that NHC

169 blood levels were safely reached in humans that exceed antiviral concentrations against SARS-CoV-2 in

170 primary human airway epithelia cultures (NHC EC_{90} approx. 0.5-1 μM[9]). Our PK profiles for MK-

171 4482/EIDD-2801 revealed that NHC plasma concentrations $\geq$0.5 μM at trough (12 hours after dosing

172 based on a *b.i.d.* regimen) are reached after oral dose levels of approximately 130 mg/kg and 10 mg/kg

173 in cynomolgus macaques and ferrets, respectively[4]. These calculations drove our decision to dose ferrets

174 at the 5 mg/kg level in this study, which represents a conservative estimate of a safe human dose

175 equivalent based on all available information. By coincidence, 5 mg/kg is close to the lowest efficacious

176   dose of MK-4482/EIDD-2801 against seasonal and pandemic influenza viruses in ferrets[4,6],

177   underscoring the high broad-spectrum antiviral potential of the drug.

178   Closely resembling our prior experience with influenza therapy[4,6], MK-4482/EIDD-2801 was well

179   tolerated and orally efficacious against SARS-CoV-2, reducing upper respiratory virus load below

180   detection level within 24 hours of first drug administration when therapy was initiated after the onset of

181   virus shedding, and by nearly two orders of magnitude when first administered at the peak of virus

182   replication. Viral genetic material in gastrointestinal samples was likewise undetectable in treated

183   animals, which is consistent with previous observations of sustained presence of the biologically active

184   triphosphate form of NHC in all soft tissue but liver in different species[4,8,29].

185   Importantly, treatment suppressed all transmission to untreated direct contacts, despite prolonged

186   direct proximity of source and contact animals and detectable virus shedding from source animals at the

187   beginning of the co-housing phase. This complete transmission block may indicate a bottom threshold of

188   shed SARS-CoV-2 load for successful spread. Since the antiviral effect of NHC arises from induction of

189   error catastrophe[4,7,8], it is also possible that genome integrity of some EIDD-2801-experienced virions

190   shed from treated animals was only partially compromised. Incorporated NHC base pairs as cytosine or

191   uracil due to spontaneous tautomeric interconversions[30]. Limited presence of the analog in viral

192   genomes generated shortly after treatment start could have still allowed virus replication on cultured

193   cells for titration, but not successful host invasion.

194   Our prior studies with influenza viruses demonstrate that the MK-4482/EIDD-2801-mediated block

195   of respiratory viral transmission is not host species-restricted. Oral treatment with MK-4482/EIDD-2801

196   or NHC reduced shed influenza virus titers in ferret nasal lavages with potency and kinetics comparable

197   to the effect seen here against SARS-CoV-2[4] and effectively prevented influenza virus direct contact

198   transmission between guinea pigs[7]. If ferret-based inhibition of SARS-CoV-2 transmission by MK-

199   4482/EIDD-2801 is predictive of the antiviral effect in humans, COVID-19 patients could become non-

200   infectious within 24 to 36 hours after the onset of oral treatment. In addition to the direct therapeutic

201   promise of alleviating clinical disease, a shortened shedding period would safely allow reduction of

202   isolation times of SARS-CoV-2 positives and narrow the window of opportunity for viral transmission.

203   Treatment with MK-4482/EIDD-2801, in particular when initiated early after infection, thus has the

204   potential to provide three-fold benefit: it may mitigate the risk of progression to severe disease and

205   accelerate recovery, ease the emotional and socioeconomic toll associated with mandatory prolonged

206   isolation, and aid in rapidly silencing local outbreaks.

207

Main References

209   1   Rodriguez Mega, E. COVID has killed more than one million people. How many more will die?
210   *Nature*, doi:10.1038/d41586-020-02762-y (2020).
211   2   Martinot, M. *et al.* Remdesivir failure with SARS-CoV-2 RNA-dependent RNA-polymerase
212   mutation in a B-cell immunodeficient patient with protracted Covid-19. *Clin. Infect. Dis.*,
213   doi:10.1093/cid/ciaa1474 (2020).
214   3   Humeniuk, R. *et al.* Safety, Tolerability, and Pharmacokinetics of Remdesivir, An Antiviral for
215   Treatment of COVID-19, in Healthy Subjects. *Clin. Transl. Sci.* **13**, 896-906,
216   doi:10.1111/cts.12840 (2020).
217   4   Toots, M. *et al.* Characterization of orally efficacious influenza drug with high resistance barrier
218   in ferrets and human airway epithelia. *Sci. Transl. Med.* **11**, doi:10.1126/scitranslmed.aax5866
219   (2019).
220   5   Toots, M. & Plemper, R. K. Next-generation direct-acting influenza therapeutics. *Transl. Res.*,
221   doi:10.1016/j.trsl.2020.01.005 (2020).
222   6   Toots, M. *et al.* Quantitative efficacy paradigms of the influenza clinical drug candidate EIDD-
223   2801 in the ferret model. *Transl. Res.* **218**, 16-28, doi:10.1016/j.trsl.2019.12.002 (2020).
224   7   Yoon, J. J. *et al.* Orally Efficacious Broad-Spectrum Ribonucleoside Analog Inhibitor of
225   Influenza and Respiratory Syncytial Viruses. *Antimicrob. Agents Chemother.* **62**,
226   doi:10.1128/AAC.00766-18 (2018).
227   8   Urakova, N. *et al.* beta-d-N (4)-Hydroxycytidine Is a Potent Anti-alphavirus Compound That
228   Induces a High Level of Mutations in the Viral Genome. *J. Virol.* **92**, doi:10.1128/JVI.01965-17
229   (2018).
230   9   Sheahan, T. P. *et al.* An orally bioavailable broad-spectrum antiviral inhibits SARS-CoV-2 in
231   human airway epithelial cell cultures and multiple coronaviruses in mice. *Sci. Transl. Med.* **12**,
232   doi:10.1126/scitranslmed.abb5883 (2020).
233   10   Han, K. *et al.* Lung Expression of Human ACE2 Sensitizes the Mouse to SARS-CoV-2
234   Infection. *Am. J. Respir. Cell Mol. Biol.*, doi:10.1165/rcmb.2020-0354OC (2020).

235   11   Salajegheh Tazerji, S. *et al.* Transmission of severe acute respiratory syndrome coronavirus 2
236   (SARS-CoV-2) to animals: an updated review. *J. Transl. Med.* **18**, 358, doi:10.1186/s12967-020-
237   02534-2 (2020).
238   12   Oreshkova, N. *et al.* SARS-CoV-2 infection in farmed minks, the Netherlands, April and May
239   2020. *Euro Surveill.* **25**, doi:10.2807/1560-7917.ES.2020.25.23.2001005 (2020).
240   13   Enserink, M. Coronavirus rips through Dutch mink farms, triggering culls. *Science* **368**, 1169,
241   doi:10.1126/science.368.6496.1169 (2020).
242   14   Oude Munnink, B. B. *et al.* Jumping back and forth: anthropozoonotic and zoonotic transmission
243   of SARS-CoV-2 on mink farms. *bioRxiv*, 2020.2009.2001.277152,
244   doi:10.1101/2020.09.01.277152 (2020).
245   15   Bruschke, C.   (ed Nature and Food Quality Ministry of Agriculture) (2020).
246   16   Schlottau, K. *et al.* SARS-CoV-2 in fruit bats, ferrets, pigs, and chickens: an experimental
247   transmission study. *Lancet Microbe* **1**, e218-e225, doi:10.1016/S2666-5247(20)30089-6 (2020).
248   17   Richard, M. *et al.* SARS-CoV-2 is transmitted via contact and via the air between ferrets. *Nat*
249   *Commun* **11**, 3496, doi:10.1038/s41467-020-17367-2 (2020).
250   18   Davies, N. G. *et al.* Age-dependent effects in the transmission and control of COVID-19
251   epidemics. *Nat. Med.* **26**, 1205-1211, doi:10.1038/s41591-020-0962-9 (2020).
252   19   Hartman, A. L. *et al.* SARS-CoV-2 infection of African green monkeys results in mild
253   respiratory disease discernible by PET/CT imaging and shedding of infectious virus from both
254   respiratory and gastrointestinal tracts. *PLoS Pathog.* **16**, e1008903,
255   doi:10.1371/journal.ppat.1008903 (2020).
256   20   Shi, J. *et al.* Susceptibility of ferrets, cats, dogs, and other domesticated animals to SARS-
257   coronavirus 2. *Science* **368**, 1016-1020, doi:10.1126/science.abb7015 (2020).
258   21   Rosenke, K. *et al.* Defining the Syrian hamster as a highly susceptible preclinical model for
259   SARS-CoV-2 infection. *bioRxiv*, doi:10.1101/2020.09.25.314070 (2020).
260   22   Bertzbach, L. D. *et al.* SARS-CoV-2 infection of Chinese hamsters (Cricetulus griseus)
261   reproduces COVID-19 pneumonia in a well-established small animal model. *Transbound.*
262   *Emerg. Dis.*, doi:10.1111/tbed.13837 (2020).
263   23   Imai, M. *et al.* Syrian hamsters as a small animal model for SARS-CoV-2 infection and
264   countermeasure development. *Proc. Natl. Acad. Sci. U. S. A.* **117**, 16587-16595,
265   doi:10.1073/pnas.2009799117 (2020).
266   24   Newman, A. *et al.* First Reported Cases of SARS-CoV-2 Infection in Companion Animals - New
267   York, March-April 2020. *MMWR Morb. Mortal. Wkly. Rep.* **69**, 710-713,
268   doi:10.15585/mmwr.mm6923e3 (2020).
269   25   Sit, T. H. C. *et al.* Infection of dogs with SARS-CoV-2. *Nature*, doi:10.1038/s41586-020-2334-5
270   (2020).
271   26   Li, X. *et al.* Clinical laboratory characteristics of severe patients with coronavirus disease 2019
272   (COVID-19): A systematic review and meta-analysis. *Clin Epidemiol Glob Health*,
273   doi:10.1016/j.cegh.2020.08.012 (2020).
274   27   Huang, I. & Pranata, R. Lymphopenia in severe coronavirus disease-2019 (COVID-19):
275   systematic review and meta-analysis. *J Intensive Care* **8**, 36, doi:10.1186/s40560-020-00453-4
276   (2020).
277   28   in *GEN Genetic Engineering & Biotechnology News*   (2020).
278   29   Painter, G. R. *et al.* The prophylactic and therapeutic activity of a broadly active ribonucleoside
279   analog in a murine model of intranasal venezuelan equine encephalitis virus infection. *Antiviral*
280   *Res.* **171**, 104597, doi:10.1016/j.antiviral.2019.104597 (2019).

281   30   Les, A., Adamowicz, L. & Rode, W. Structure and conformation of N4-hydroxycytosine and N4-
282   hydroxy-5-fluorocytosine. A theoretical ab initio study. *Biochim. Biophys. Acta* **1173**, 39-48,
283   doi:10.1016/0167-4781(93)90240-e (1993).
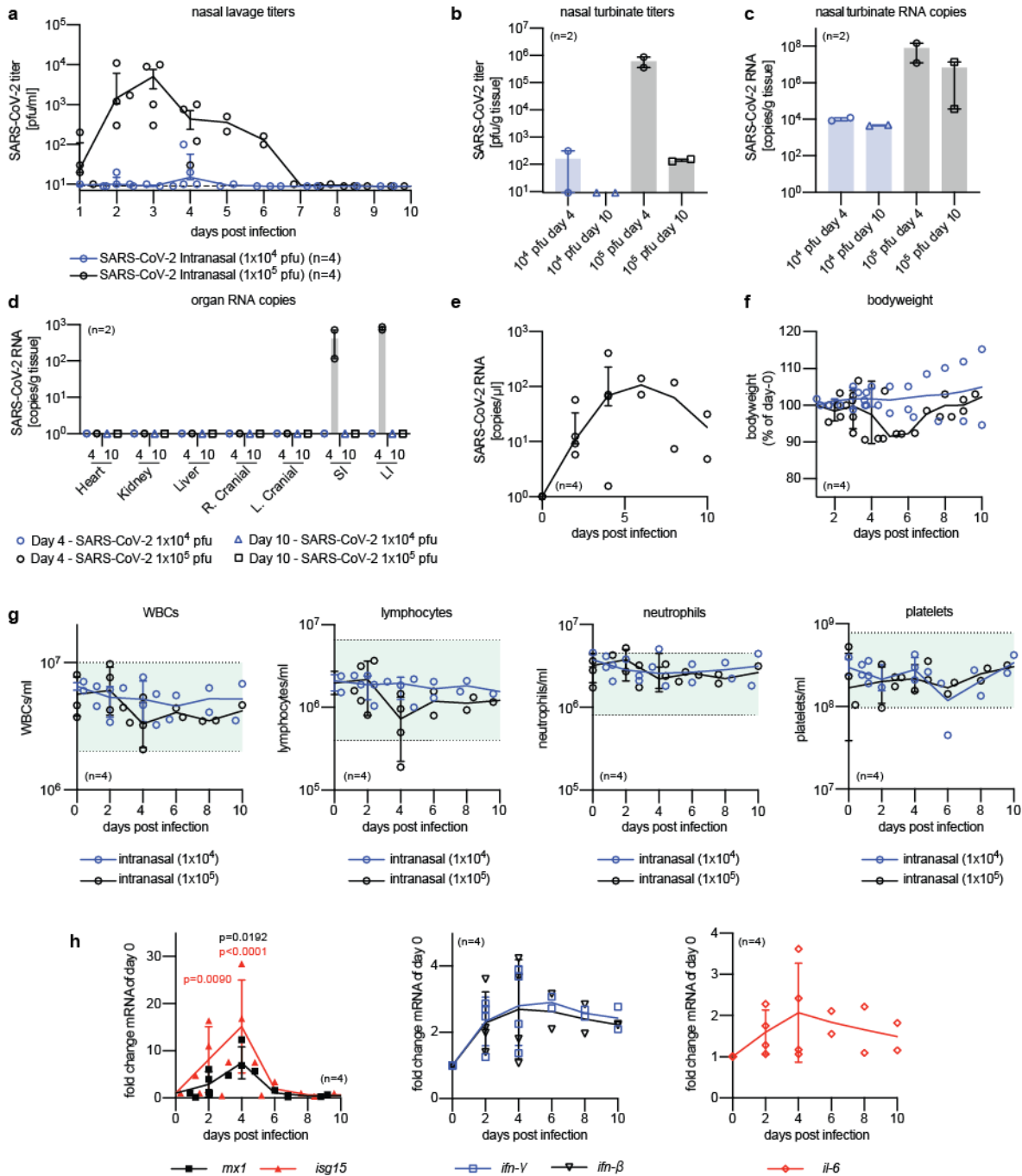
284

285 **Fig. 1. SARS-CoV-2 infects the upper respiratory tract of ferrets.** Ferrets (n=4) were inoculated

286 intranasally with 1×10^4 or 1×10^5 pfu of 2019-nCoV/USA-WA1/2020. **a**, Virus titer in nasal lavages

287 collected daily. **b-f**, At 4 and 10 days post infection, 2 ferrets were sacrificed in each group and infection

288 was characterized. **b,** Infectious virus particles in nasal turbinates. **c,** Viral RNA was present in the nasal

289   turbinates of all infected ferrets. **d**, RT-qPCR quantitation of viral RNA copies in selected organs, two

290   lung lobes (right (R.) and left (L.) cranial) per animal, and small (SI) and large (LI) intestine samples

291   extracted from infected ferrets four or 10 days after infection. **e,** Detection of 2019-nCoV/USA-

292   WA1/2020 RNA in rectal swabs of ferrets inoculated with 1×10^5 pfu. **f,** Bodyweight of ferrets, measured

293   daily and expressed as % of weight at day 0. **g**, Complete blood count analysis, performed every second

294   day. No noticeable differences were detected for all parameters tested, including total WBCs,

295   lymphocytes, neutrophils, and platelets. The shaded green areas represent normal Vetscan HM5 lab

296   values. **h**, Selected interferon and cytokine responses in PBMCs harvested every two days after

297   infection. Analysis by qPCR for animals infected with 1×10^5 pfu of 2019-nCoV/USA-WA1/2020.

298   Infected ferrets displayed elevated expression of interferon stimulated genes (*mx1* and *isg15* (h; left)),

299   *ifn-β* and *ifn-γ* (h; center), and *il-6* (h; right). Statistical analysis by two-way ANOVA with Dunnett's

300   post-hoc multiple comparison test. In all panels, symbols represent independent biological repeats

301   (individual animals), lines connect group medians ± SEM (a,e) or SD (f-h), and bar graphs (b-d) show

302   means ± range.

303
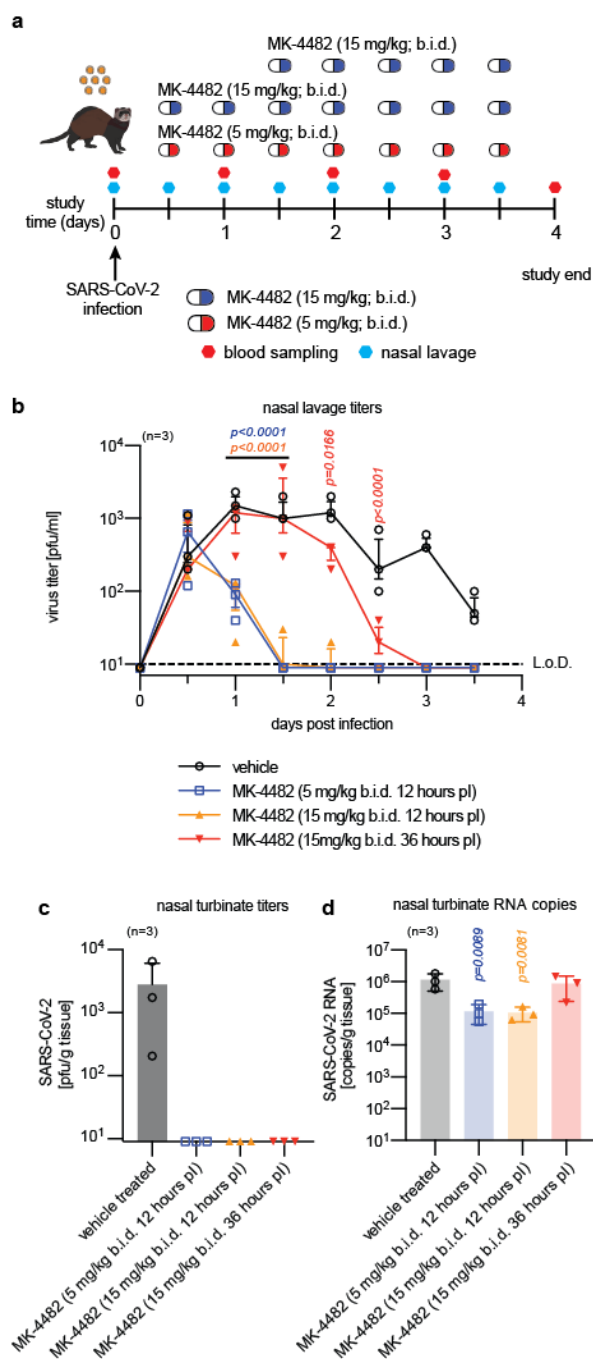
Fig. 2. Therapeutic MK-4482/EIDD-2801 is orally efficacious against SARS-CoV-2 in ferrets. a,

Therapeutic efficacy study schematic. Ferrets (n=3) were infected intranasally with 1×10^5 pfu 2019-

nCoV/USA-WA1/2020 and either gavaged with vehicle or treated *b.i.d.* with MK-4482/EIDD-2801

commencing 12 (5 mg/kg and 15 mg/kg) or 36-hours (15 mg/kg) after infection. Nasal lavages were

collected twice daily. Blood was collected every other day. **b,** Viral nasal lavage titers in infected ferrets

309   from (a). Treatment with MK-4482/EIDD-2801 significantly reduced virus titers within 12 hours dosing

310   onset in all treatment groups. Statistical analysis by two-way ANOVA with Dunnett's multiple

311   comparison post-hoc test. P values are shown. **c-d,** Quantitation of infectious particles (c) and virus

312   RNA copy numbers (d) in nasal turbinates of infected ferrets extracted four days after infection.

313   Statistical analysis by one-way ANOVA with Dunnett's multiple comparison post-hoc test. P values are

314   shown. In all panels, symbols represent independent biological repeats (individual animals), lines

315   connect group medians ± SEM (b), and bar graphs (c-d) show means ± SD.
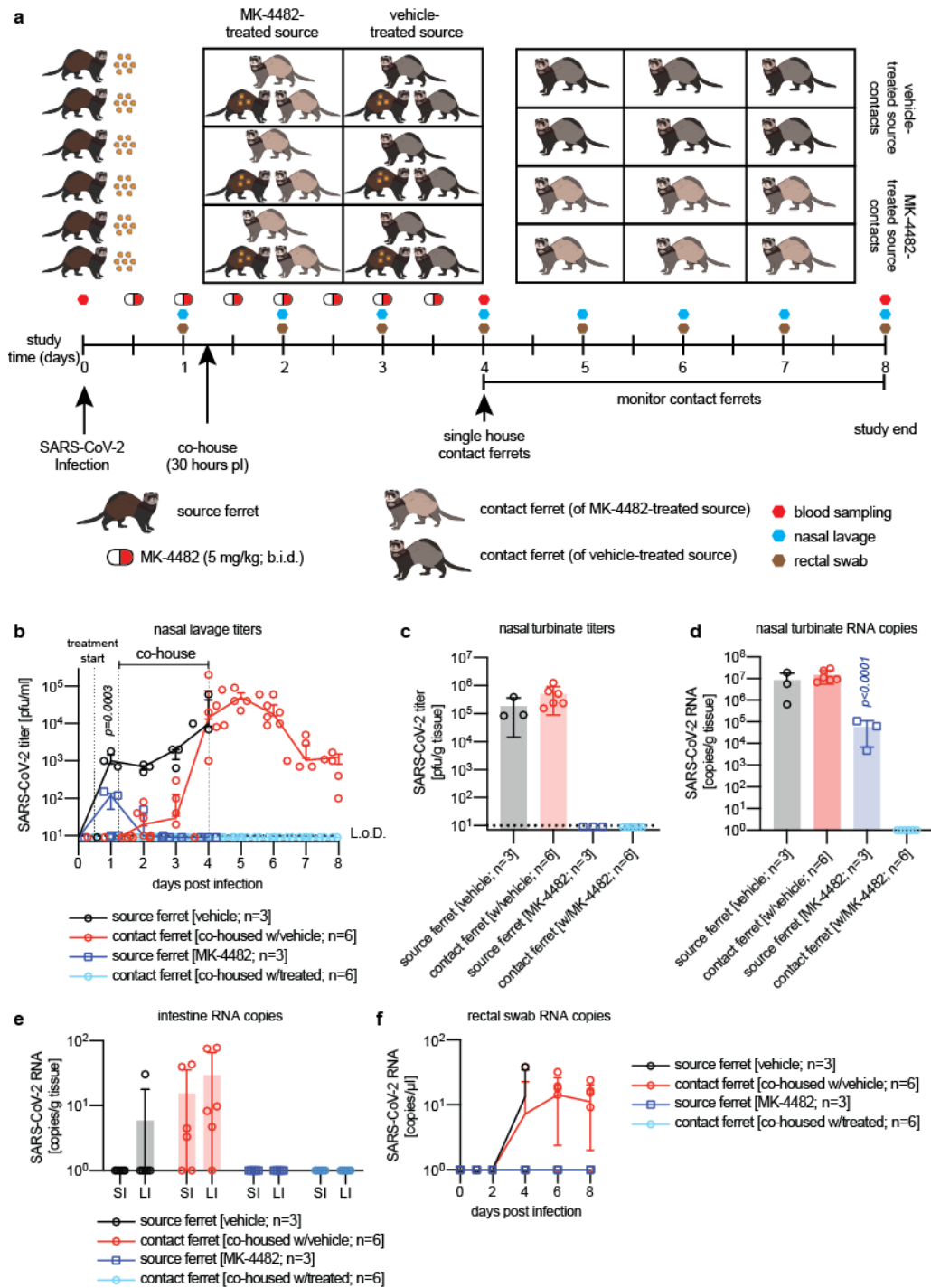
Fig. 3. Therapeutic oral treatment with MK-4482/EIDD-2801 prevents contact transmission. a,
Contact transmission study schematic. Two groups of source ferrets (n=3 each) were infected with
1×10^5 pfu of 2019-nCoV/USA-WA1/2020 and received MK-4482/EIDD-2801 treatment (5 mg/kg
b.i.d.) or vehicle starting 12 hours after infection. At 30 hours after infection, each source ferret was co-

321   housed with two uninfected, untreated contact ferrets. After three days, source animals were euthanized

322   and contact ferrets isolated and monitored for four days. Nasal lavages and rectal swabs were collected

323   once daily and blood sampled at 0, 4, and 8 days post infection. **b**, Source ferrets treated with MK-

324   4482/EIDD-2801 had significantly lower virus titers 12 hours after treatment onset (p=0.0003) than

325   vehicle animals. Contacts of vehicle-treated sources began to shed 2019-nCoV/USA-WA1/2020 within

326   20 hours of co-housing. No virus was detectable in untreated contact of MK-4482/EIDD-2801-treated

327   source ferrets. Statistical analysis by two-way ANOVA with Sidak's multiple comparison post-hoc test.

328   P values are shown. **c-d,** Quantitation of infectious particles (c) and virus RNA copy numbers (d) in

329   nasal turbinates of source and contact ferrets from (b), extracted four and eight days after study start,

330   respectively. Statistical analysis by one-way ANOVA with Sidak's multiple comparison post-hoc test. **e-**

331   **f,** Quantitation of virus RNA copy numbers in small (SI) and large (LI) intestines (e) and rectal swabs

332   (f). Samples of MK-4482/EIDD-2801-treated source ferrets and their contacts were PCR-negative for

333   viral RNA. In all panels, symbols represent independent biological repeats (individual animals), lines

334   connect group medians ± SEM (b) or SD (f), and bar graphs (c-e) show means ± SD.

335

336   **Methods**

337   **Study design**

338   Ferrets were used as an *in vivo* model to examine efficacy of therapeutically administered oral MK-

339   4482/EIDD-2801 against SARS-CoV-2 infection and virus transmission to uninfected contact animals.

340   Viruses were administered to source animals through intranasal inoculation and virus load monitored

341   periodically in nasal lavages and rectal swabs, and 4 or 10 days after exposure in respiratory tissues and

342   a subset of organs. Virus titers were determined based on plaque assay and viral RNA copy numbers,

343 blood samples subjected to CBC analysis and RT-qPCR quantitation of selected cytokine and innate

344 antiviral effector expression levels.

Cells and viruses

346 Vero-E6 cells were cultured in Dulbecco's modified Eagle's medium (DMEM) supplemented with

347 7.5% heat inactivated fetal bovine serum (FBS) at 37°C with 5% CO_2. SARS-CoV-2 (SARS-CoV-

348 2/human/USA-WA1/2020) was propagated using Vero-E6 cells supplemented with 2% FBS. Virus

349 stocks were stored at -80°C and titers were determined by plaque assay. Vero-E6 cells were routinely

350 checked in 6-month intervals for bacterial and mycoplasma contamination.

Plaque assay

352 Samples were serially diluted (10-fold starting at 1:10 initial dilution) in DMEM supplemented with

353 2% FBS containing antibiotics-antimycotics (Gibco). Serial dilutions were added to Vero-E6 cells

354 seeded in 12-well plates at 3×10^5 cells per well 24-hours prior. Virus was allowed to adsorb for 1 hour at

355 37°C. Subsequently, inoculum was removed, and cells were overlaid with 1.2% Avicel (FMC

356 biopolymer) in DMEM and incubated for three days at 37°C with 5% CO_2. Avicel was removed and

357 cells were washed once with PBS, fixed with 10% neutral buffered formalin, and plaques were

358 visualized using 1% crystal violet.

Establishing infectious dose

360 Female ferrets (6-10 months of age) were purchased from Triple F Farms. Upon arrival, ferrets were

361 rested for one week, then randomly assigned to groups and housed individually in ventilated negative

362 pressure cages in an ABSL-3 facility. In order to establish a suitable inoculum for efficacy and

363 transmission studies, ferrets (n=4) were inoculated intranasally with 1×10^4 and 1×10^5 pfu of 2019-

364 nCoV/USA-WA1/2020 in 1 ml (0.5 ml per nare). Prior to inoculation, ferrets were anesthetized with

365 dexmedetomidine/ketamine. Nasal lavages were performed once daily using 1 ml of PBS containing $2\times$

366 antibiotics-antimycotics (Gibco). For blood sampling, ferrets were anesthetized with dexmedetomidine

367 and approximately 0.5 ml blood was drawn from the anterior vena cava. Complete blood counts (CBC)

368 were performed using a Vetscan HM5 (Abaxis) in accordance with the manufacturer's protocol. Rectal

369 swabs were performed every two days. Groups of two ferrets were sacrificed 4- and 10-days post

370 infection and organs were harvested to determine virus titer and the presence of viral RNA in different

371 tissues.

372 ***In vivo* efficacy of MK-4482/EIDD-2801 in ferrets**

373   Groups of ferrets (n=3 each) were inoculated with 1×10^5 pfu of 2019-nCoV/USA-WA1/2020 in 1

374 ml (0.5 ml per nare). At 12 hours after infection, three groups of ferrets were treated *b.i.d.* with vehicle

375 (1% methylcellulose) or MK-4482/EIDD-2801 at a dose level of 5 mg/kg or 15 mg/kg, respectively. At

376 36 hours after infection, a fourth group of ferrets began receiving *b.i.d.* treatment with MK-4482/EIDD-

377 2801 at a dose of 15 mg/kg. Compound was administered via oral gavage in 1% methylcellulose. After

378 treatment onset, *b.i.d.* dosing was continued until four days after infection. Nasal lavages were

379 performed on all ferrets every 12 hours. Blood samples were obtained every two days after infection and

380 stored in K_2-EDTA tubes (Sarstedt CB 300). CBC analysis was performed on each blood sample in

381 accordance with the manufacturer's protocols. After CBC analysis, red blood cells were lysed with ACK

382 buffer (150 mM NH_4CL, 10mM $KHCO_3$, 0.01 mM EDTA pH 7.4) and PBMCs were harvested and

383 stored at -80°C in RNAlater until further qPCR analysis was performed. Four days after infection, all

384 ferrets were euthanized and organs harvested to determine virus titers and the presence of viral RNA in

385 different tissues.

386 **Contact transmission of SARS-CoV-2 in ferrets**

387   A group of 6 individually housed source ferrets were inoculated intranasally with 1×10^5 pfu of

388 2019-nCoV/USA-WA1/2020. Twelve hours after infection, source ferrets were split into two groups

389   (n=3 each) receiving vehicle or MK-4482/EIDD-2801 treatment at a dose of 5 mg/kg *b.i.d.* daily by oral

390   gavage. At 30 hours post infection, each source ferret was co-housed with two uninfected and untreated

391   contact ferrets. Ferrets were co-housed until 96 hours after infection, when source ferrets were

392   euthanized and contact animals housed individually. Contact animals were monitored for four days after

393   separation from source ferrets, then sacrificed. Nasal lavages and rectal swabs were performed every 24

394   hours on all ferrets. Blood samples were collected at 0, 4, and 8 days after source ferret infection. For all

395   ferrets, organs were harvested to determine virus titers and the presence of viral RNA in different

396   tissues.

397   **Titration of SARS-CoV-2 in tissue extracts**

398   For virus titration, organs were weighed and homogenized in PBS. Homogenates were centrifuged

399   for 5 minutes at 2,000×g at 4°C. Clarified supernatants were harvested and used in subsequent plaque

400   assays. For detection of viral RNA, harvested organs were stored in RNAlater at -80°C. Tissues were

401   ground and total RNA was extracted using a RNeasy mini kit (Qiagen). RNA was extracted from rectal

402   swabs using the ZR Viral RNA Kit (Zymo Research) in accordance with the manufacturer's protocols.

403   **SARS-CoV-2 RNA copy numbers**

404   Detection of SARS-CoV-2 RNA was performed using the nCoV_IP2 primer-probe set (National

405   Reference Center for Respiratory Viruses, Institut Pasteur, Paris) targeting the SARS-CoV-2 RdRp

406   gene. An Applied Biosystems 7500 Real-Time PCR System using the StepOnePlus Real-Time PCR

407   System was used to perform qPCR reactions. TaqMan Fast Virus 1-Step Master Mix (Thermo Fisher

408   Scientific) was used in combination with the nCoV_IP2 primer-probe set to detect viral RNA. To

409   quantitate RNA copy numbers, a standard curve was created using a PCR fragment (nucleotides 12669-

410   14146 of the SARS-CoV-2 genome) generated from viral cDNA using nCoV_IP2 forward primer and

411   the nCoV_IP4 reverse primer. RNA values were normalized based on weights of tissues used.

412   **Systemic interferon and cytokine profiling**

413   Relative expression of interferon, interferon stimulated genes and cytokines was determined by real-

414   time PCR analyses. RNA was extracted from PBMCs harvested at various after infection. cDNA was

415   reverse transcribed with SuperScript III (Invitrogen) using oligo-dT primers and analyzed by real-time

416   PCR using Fast SYBR Green Master Mix (Applied Biosystems). Signals were normalized to

417   glyceraldehyde-3-phosphate dehydrogenase mRNA, analyzed by the comparative threshold cycle

418   ($\Delta\Delta$Ct) method, and expressed relative to day 0 of infection for each respective animal. Sequences of the

419   primers used for the analyses are shown in supplementary table S1.

420   **Statistical analysis**

421   When comparing more than two groups, one-way analysis of variance (ANOVA) or two-way

422   ANOVA with Dunnett's or Sidak's multiple comparison post hoc tests as specified in figure legends

423   were used to assess statistical difference between samples. All statistical analyses were carried out in

424   Prism version 8.4.3 (GraphPad). The number of individual biological replicates (n values) is shown in

425   the figures and specified in the figure legends for each experiment. Representations of mean or median $\pm$

426   standard deviation are specified in the figure legends. The significance threshold (α) was set to 0.05.

427   Exact P values are provided in the figures.

428   **Ethical compliance**

429   All animal work was performed in compliance with the *Guide for the Care and Use of Laboratory*

430   *Animals* of the National Institutes of Health and the Animal Welfare Act Code of Federal Regulations.

431   Experiments with SARS-CoV-2 involving ferrets were approved by the Georgia State Institutional

432   Animal Care and Use Committee under protocol A20031. All experiments using infectious SARS-CoV-

433   2 were approved by the Georgia State Institutional Biosafety Committee under protocol B20016 and

434   performed in a BSL-3/ABSL-3 facilities at Georgia State University.

435

Acknowledgements

Author Contributions

RMC and JDW performed virus stock preparations, animal inoculation, sampling and necropsies, contributed to experiment design, data analysis and presentation, and edited the manuscript. RMC performed all RT-qPCR experiments and analyses. JDW performed all CBC analyses. RKP conceived, designed and coordinated the study, conceived and designed experiments, contributed to animal inoculation and necropsies, contributed to data analysis and presentation, and wrote the manuscript.

Competing Interests Declaration

The authors declare no competing interests.

Additional information

Supplementary Information

Supplementary Information is available for this paper.

457

458   **Correspondence**

459   Correspondence and requests for materials should be addressed to Richard K Plemper.

460

461   **Data Availability**

462   All data generated or analyzed during this study are included in this published article (and its

463   supplementary information files). Source data for figures 1-3 and extended data figures 1-3 are provided

464   with the paper in supplementary data file 1.

465

466   **Code Availability**

467   This study does not use custom codes. All commercial computer codes and algorithms used are

468   specified in the Methods section.

469
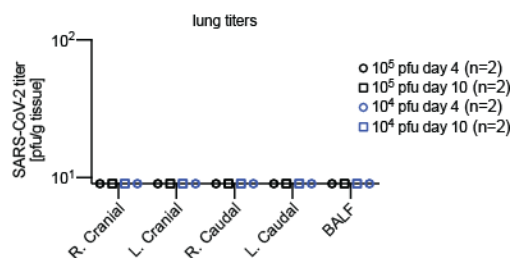
470

471   **Extended Data Fig. 1. SARS-CoV-2 does not progress to the ferret lower respiratory tract. a,**

472   Analysis of bronchioalveolar lavages (BALF) and four lung lobes (right (R.) and left (L.) cranial and

473   caudal) per ferret. BALF and tissues samples were harvested 4 (n=2) and 10 (n=2) days after infection.

474   Symbols represent independent biological repeats (individual animals).
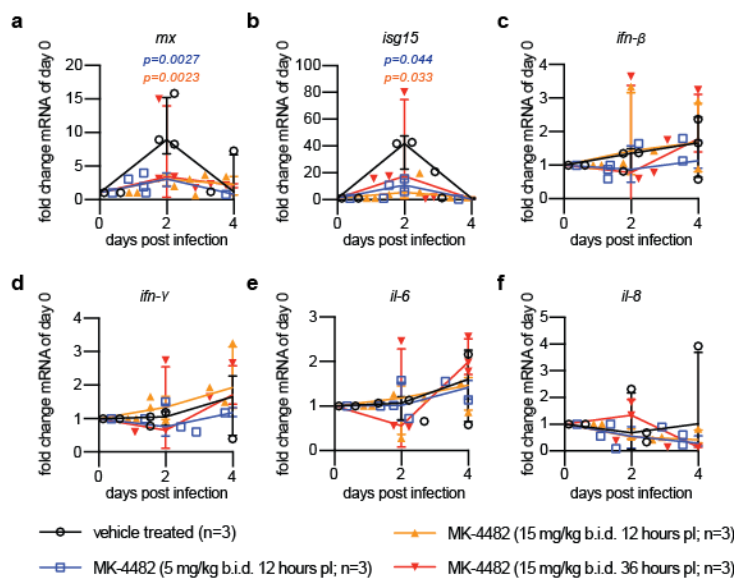
Extended Data Fig. 2. Interferon induction and cytokine profiling of SARS-CoV-2 ferrets treated with MK-4482/EIDD-2801. a-f, Selected interferon and cytokine expression levels in PBMCs relative to day 0. Blood samples of animals treated with MK-4482/EIDD-2801 or vehicle as specified were collected every two days after infection and PBMCs analyzed by RT-qPCR. Statistical analysis of changes relative to day 0 by two-way ANOVA with Dunnett's post-hoc multiple comparison test. In all panels, symbols represent independent biological repeats (individual animals), lines connect group medians ± SD.
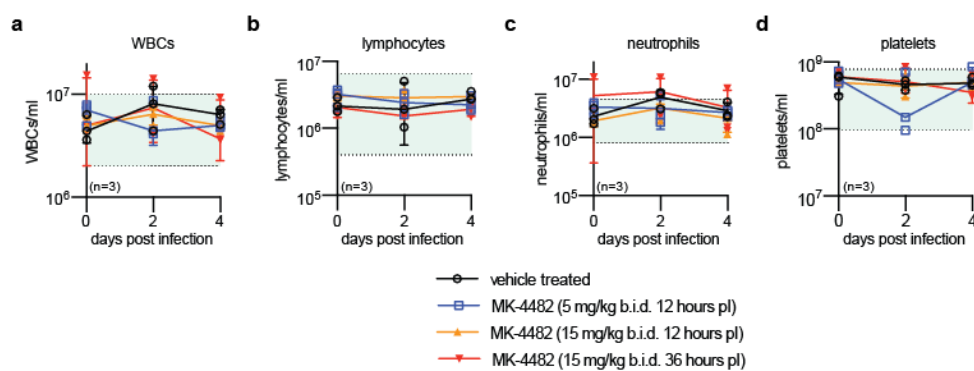
Extended Data Fig. 3. Complete blood count of SARS-CoV-2 ferrets treated with MK-4482/EIDD-2801. a-d, Blood samples were collected every two days after infection and complete blood counts determined. No abnormal values were observed in all parameters tested, including total WBCs (a),

487   lymphocytes (b), neutrophils (c), and platelets (d). The shaded green areas represent normal Vetscan

488   HM5 lab values. Symbols represent independent biological repeats (individual animals), lines connect

489   group medians ± SD.